jove

Micropatterned Magneto-Rheological Elastomers to Drive Changes in Cardiomyocyte Alignment

Ali H. Lateef[1], **Nesrine Bouhrira**[2], **Jia-Jye Lee**[2], **Alexia Vite**[2], **Kenneth B. Margulies**[2], **Elise A. Corbin**[1,3,4]

[1] Department of Biomedical Engineering, University of Delaware [2] Cardiovascular Institute, Perelman School of Medicine, University of Pennsylvania [3] Department of Materials Science and Engineering, University of Delaware [4] Nemours/Alfred I. duPont Hospital for Children

Corresponding Author

Elise A. Corbin
ecorbin@udel.edu

Citation

Lateef, A.H., Bouhrira, N., Lee, J.J., Vite, A., Margulies, K.B., Corbin, E.A. Micropatterned Magneto-Rheological Elastomers to Drive Changes in Cardiomyocyte Alignment. *J. Vis. Exp.* (220), e68271, doi:10.3791/68271 (2025).

Date Published

June 10, 2025

DOI

10.3791/68271

URL

jove.com/video/68271

Abstract

Substrate-associated cues, such as mechanical and topographic, profoundly influence cellular response. However, much of the foundational research employs static or isolated effects. The direction and timescale of these mechanical effects on emergent cellular responses remain largely unexplored. Tools to examine how time-varying substrate-associated stimuli drive physiological and pathological processes can unlock the next level of mechanobiological insight. Here, we use micro-patterned magnetorheological elastomers (MREs) that can rapidly stiffen and soften in response to an external magnetic field, allowing for a more rigorous investigation of the effects of mechanical (stiffness) and contact-guided (topographic) stimulation on neonatal rat cardiomyocyte orientation and alignment. By integrating dynamic control of mechanical stiffness that can be temporally tuned and reversed, we can rigorously test the effects of load by (1) pre-conditioning under identical conditions and (2) acutely changing *in vitro* biomechanics to mimic clinically relevant phenomenology, such as myocardial infarction properly. This approach allows us to study the impact of load on cellular responses in a more realistic and controlled manner.

Introduction

The heart's ability to pump blood efficiently relies on the architecture and mechanical properties (stiffness) of its myocardium, where the precise organization of cells and tissue is essential for coordinated contraction and overall function. The myocardium is primarily composed of cardiomyocytes (CMs), which, in adults, exhibit an elongated, almost rod-like morphology with sarcomeres (the contractile unit of the CMs) aligned along the length of the cell. In contrast, fetal or induced pluripotent stem cell (iPSC)-derived CMs differ significantly from adult CMs. They tend to have a more rounded shape, a single nucleus, a disorganized or unaligned sarcomeric structure, and an irregular beating frequency. The structural resemblance of the *in vivo* organization of the myocardium allows for synchrony of contraction and force transmission; this is critical and essential to recapitulating natural myocardium

through an *in vitro* model. To generate CMs with structural characteristics similar to mature myocardium, previous studies have demonstrated successful strategies for enhancing maturation, including manipulating substrate stiffness[1,2], applying mechanical strain[3], utilizing contact guidance[4,5], or employing electrical pacing[6,7].

It has long been understood that the stiffness of the extracellular environment impacts cells. A vast diversity of stiffness exists throughout the human body, ranging from hundreds of pascals (Pa) in the brain and up to tens of gigapascals (GPa) in bone[8,9,10]. It has been found that during development, tissues change stiffness, and this alteration regulates cellular level differentiation and maturation into the adult phenotypes that are needed for normal function[11,12,13,14]. Changes in stiffness have also been linked to disease states and the progression of specific pathologies[15,16,17,18]. Specifically, the stiffness of the myocardium changes with the development and progression of diseases; for instance, a healthy myocardium has an elastic modulus of ~10 kPa in contrast to a failing heart, which has an elastic modulus of 35-70 kPa or more[19]. Additionally, numerous *in vitro* studies have reported that cardiomyocytes cultured on a substrate similar to the native myocardium stiffness had better sarcomere organization[20], generated optimal contraction[1,19], and had the longest action potential duration[21].

Additionally, it has become more well-recognized that cells *in vivo* are exposed to a complex variety of topographical cues within their microenvironment that drive form and function. These topographical cues come in various sizes and geometries, from the random arrangement of integrins at a molecular level to the micron-level alignment of cells in muscle tissues[22,23]. Similar to other mechanical regulators, topography is important to cell morphology, such as spreading, elongation, alignment, motility, differentiation, and apoptosis[24,25,26]. With the introduction of synthetic culture substrates, methods have been developed to create controlled surface topography for cell and tissue culture[27,28,29]. For instance, micropatterned nano- and micro-grooves have been used to provide contact guidance for mammalian cells so that cells orient and remodel their cytoskeleton to follow the topographical structures of the culture substrate.

Here, we introduce an *in vitro* culture method that integrates both structural (contact cue) and mechanical (stiffness) guidance using a patterned magnetorheological elastomer (MRE) substrate, a tunable material that can be stiffened or softened by adjusting the strength of the magnetic field[17,30,31,32]. By positioning magnets near the culture substrate, stiffness can be increased, with the degree of stiffening modifiable by varying the distance between the sample and the magnet. Conversely, stiffness can be reduced by removing the magnet altogether. This approach provides a robust, dynamic, and controllable method to replicate the *in vivo*-like mechanical conditions, while the surface micropatterning introduces anisotropy, enabling the creation of more biomimetic 2D cell culture substrates.

Protocol

1. Preparation of patterned PDMS stamp

NOTE: A PDMS stamp is essential for its flexibility, allowing easy manipulation and precise contact when preparing the patterned MRE surface. The stamp's flexible nature also enables effortless removal from the MRE PDMS layer without damaging the pattern, ensuring both accurate pattern transfer and preservation of the MRE surface.

1. Prepare 10 g of 10:1 (base: curing agent) 184 PDMS.
2. Pour 5 g of the 184 PDMS into a 35 mm Petri dish and degas in a desiccator for ~5-10 min, until all bubbles have dissipated.
3. Allow 184 PDMS to partially cure in an oven at 60 °C for 30 min.
4. When 5 min remains for the 184 PDMS to partially cure, add a thin layer of the extra 184 PDMS to the diffraction grating and degas in the desiccator for ~5 min.
5. Remove the 35 mm dish with the partially cured 184 PDMS from the oven.
6. Flip the diffraction grating with PDMS onto the partially cured 184 PDMS in a 35 mm dish.
   NOTE: Ensure that the diffraction grating is facing down into the partially cured 184 PDMS in the 35 mm dish.
7. Lightly press the diffraction grating until a small amount of 184 PDMS surrounds the grating.
8. Use the remaining uncured 184 PDMS to backfill the dish surrounding the grating to ensure it stays in place while curing.
9. Place the dish containing the diffraction grating into the oven set at 60 °C for 1.5 h.
10. After the 184 PDMS is fully cured, remove the 35 mm dish with the diffraction grating from the oven.
11. Score around the diffraction grating with a scalpel.
12. Apply a small amount of isopropyl alcohol (IPA) to penetrate underneath the diffraction grating.
13. Pull the grating off the 184 PDMS in the direction parallel to the patterns.
14. Remove excess 184 PDMS, leaving only the patterned section.
15. Cut the 184 PDMS stamp to the size needed.
    NOTE: This study uses a 1 cm × 1 cm stamp for the devices.

2. Surface coating of PDMS stamp

NOTE: A silane treatment creates a surface coating that prevents unwanted adhesion between PDMS layers during stamping, ensuring smooth separation and preserving the quality of the pattern transfer.

1. Silane treatment (preferred method)
   1. Place the fabricated 184 PDMS stamp in an O_2 plasma cleaner with the patterned surface facing up. Treat the PDMS surface with 45 W of O_2 plasma for 30 s.
      NOTE: Once removed from the plasma cleaner, place a lid (or cover) over the stamps immediately to ensure no debris settles on the cleaned stamps.
   2. Place 184 PDMS stamps into a desiccator in a fume hood.
   3. Tear off the lid of a microcentrifuge tube.
   4. Place the microcentrifuge tube lid next to the 184 PDMS stamps in the desiccator.
   5. Add 20 µL of trichloro(1H, 1H, 2H, 2H-perfluorooctyl) silane to the microcentrifuge tube lid.
      CAUTION: This chemical is hazardous for health and thus must only be used in a chemical fume hood.
   6. Close the desiccator and pull a vacuum.
   7. Allow the silane to coat the stamps from 1 h to overnight.

3. Preparation of magnetorheological elastomers

NOTE: To create tunable and reversible MREs, a precise ratio of carbonyl iron particles and elastomer, combined with the application of a magnetic field, enables the adjustment of stiffness across a range of values. By varying the particle fraction, base elastomer modulus, and magnetic field strength, the material's stiffness can be finely tuned to meet specific requirements.

1. Softer dynamic range MRE preparation (see **Table 1** for example weights)
    1. Measure the desired amount of silicone thinner and Eco elastomer part B and mix at 2500 rpm in a speed mixer for 1 min.
    2. Add Eco elastomer part A and carbonyl iron particles to the solution and mix at 2500 rpm in a speed mixer for 1 min.
       NOTE: The order of mixing is critical to ensure the desired polymerization timing.
    3. Using a transfer pipette with the tip cut off, add 5 g of the MRE to a new 35 mm Petri dish and degas in a desiccator for ~5 min, then allow to partially cure in the oven at 60 °C for ~10 min.
       NOTE: Ensuring that the oven and desiccator are properly leveled is essential for achieving a flat sample, which is critical for the ease of imaging.
    4. Once 5 min remain, use a transfer pipette to add extra uncured MRE to just coat the surface of the 184 PDMS stamp. Place the coated stamp in the desiccator to degas for 5 min.
       NOTE: Be careful not to use too much MRE because if it covers the edges of the stamp, it will make it more difficult to remove the stamp once the MRE is fully cured. Also, make sure to denote the direction of the pattern through every step so that when removing the stamp from the MRE, it can be pulled in the direction parallel to the patterns.
    5. Remove the MRE from the oven, and use a pair of forceps to carefully move the coated stamp. Flip it face down onto the partially cured MRE and lightly press. Put the MRE and coated stamp back into the oven at 60 °C for another 25 min.
    6. Once fully cured, use a scalpel to score the MRE at the bottom of the stamp, perpendicular to the patterns.
    7. Apply a small amount of IPA onto the cut area around the stamp.
       NOTE: The IPA should seep into the cut and start to move underneath the stamp.
    8. Using forceps, pull the stamp off the MRE in the direction parallel to the patterns.
2. Stiffer dynamic range MRE preparation (see table for example weights)
    1. Prepare 30:1 184 PDMS.
       NOTE: Make extra because some will remain stuck to the mixing container.
    2. Add the desired amount of 527 PDMS part A and part B, then carbonyl iron particles and 30:1 184 PDMS in ratios based on the example in the table.
    3. Mix it at 2500 rpm in a speed mixer for 1 min.
    4. Using a transfer pipette with the tip cut off, add 5 g of the MRE to a new 35 mm petri dish and degas in a desiccator for ~5 min, then allow to partially cure in the oven at 60 °C for ~40 min.

5. Once 5 min remain, use a transfer pipette to add extra uncured MRE to just coat the surface of the PDMS stamp. Place the coated stamp in the desiccator to degas for 5 min.
   NOTE: Be careful not to use too much MRE because if it covers the edges of the stamp, it will make it more difficult to remove the stamp once the MRE is fully cured. Also, make sure to denote the direction of the pattern through every step so that when removing the stamp from the MRE, it can be pulled in the direction parallel to the patterns.
6. Remove the MRE from the oven.
7. Use a pair of forceps to carefully move the coated stamp, flip it face down onto the partially cured MRE, and lightly press.
8. Put the MRE with the coated stamp on the top rack into the oven at 60 °C overnight.
9. Once fully cured, use a scalpel to cut the MRE at the bottom of the stamp, perpendicular to the patterns.
10. Apply IPA onto the cut area around the stamp.
    NOTE: The IPA should seep into the cut and start to move underneath the stamp.
11. Using forceps, pull the stamp off the MRE in the direction parallel to the patterns.

	Stiffness Range	Materials	Example Weight	
Softer	10–80 kPa	Eco (A+B)	11.25 g (A)	11.25 g (B)
		Silicone Thinner	22.5 g	
		Iron Particles	45 g	
Stiffer	60–120 kPa	527 PDMS (A+B)	18.75 g (A)	18.75 g (B)
		Iron Particles	37.5 g	
		184 PDMS (Base+Cure)	14.5 g (Base)	0.5 g (Cure)

Table 1: Example weights of all materials for fabricating both softer and stiffer MREs. The weights in the table are for making a total of 90 g of MRE material. Preparing less can be accomplished by mixing all constituents in the same ratios as the example weights in the table.

4. Cell culture preparation

NOTE: Cell culture preparation involves selecting the appropriate cell line, preparing culture media with necessary nutrients and growth factors, and ensuring sterile conditions to prevent contamination. Cells are plated in culture vessels and incubated at optimal conditions (usually 37 °C with controlled CO_2). Regular monitoring, medium changes, and passaging are performed to maintain healthy cell growth.

1. Sterilize the surface of the MRE by washing it with 70% ethanol 3 times and allow the third wash to sit for 20 min.

2. Wash the MRE surface 3 times with sterile phosphate-buffered saline (PBS) by adding enough volume to cover the dish completely, followed by aspirating off all liquid.
3. Coat the surface of the MRE with fibronectin (10 µg/mL) in PBS for 1 h at 37 °C to promote cell adhesion to the device.
4. Wash the MRE surface 3 times with PBS, similar to step 4.1.2.
5. Seed the neonatal rat cardiomyocytes at a density of 20,000 cells/cm^2.
6. Add magnets to the devices temporally to stiffen the matrix during the cell culture.
   NOTE: Be careful when placing devices with magnets in the incubator. The devices need to be placed far apart to guarantee that the magnets do not interact. This study recommends the usage of stainless steel-lined incubators over copper-lined incubators as there is less interaction.

5. Staining and imaging

1. Fixed cell imaging
   NOTE: Fixed cell imaging involves several key steps to visualize specific cellular components. First, cells are fixed to preserve their structure. Next, the cell membrane is permeabilized to allow stain penetration, followed by a blocking step to prevent the non-specific binding of antibodies or stains to unintended sites, such as other proteins or cellular debris. Cells are then stained with dyes or antibodies targeting specific molecules, and any excess stain is removed through washing. Finally, the stained cells are imaged using fluorescence microscopy for analysis of cellular structures.
   1. Wash once with 1x PBS by adding enough volume to cover the dish completely, followed by aspirating off all liquid.
   2. Fix cells by using 4% (v/v) paraformaldehyde for 10 min.
   3. Wash three times with 1x PBS (similar to step 5.1.1).
   4. Add 0.1% Triton X (in 1x PBS) and incubate for 5 min to permeabilize.
   5. Wash three times with 1x PBS (similar to step 5.1.1).
   6. Add NH_4Cl (50 mM in 1x PBS) and incubate for 15 min to quench.
   7. Wash three times with 1x PBS (similar to step 5.1.1).
   8. Add blocking buffer (5% BSA in 1x PBS) and incubate for 1 h at room temperature (RT).
   9. Combine the primary Anti-α-Actinin primary antibody at 1:200 into 5% BSA (in 1x PBS).
      NOTE: Mix the antibody thoroughly.
   10. Add the primary antibody solution to the sample.
      NOTE: Add enough to cover the entire sample.
   11. Incubate overnight at 4 °C.
      NOTE: Consider placing the sample on the rocker at a slow speed to help the solutions mix.
   12. Wash three times with 1x PBS (similar to step 5.1.1).
   13. Dilute the secondary antibody (555 Alexa Fluor goat anti-mouse) in 1x PBS (1:2000).
      NOTE: The secondary antibodies are light-sensitive (fluorophores). When not directly in use, make sure they are covered and out of the light.
   14. Add the secondary antibody solution to the sample.
   15. Incubate at RT for 2 h.

16. Wash three times with 1x PBS (similar to step 5.1.1).
17. Add DAPI (1 µg/mL in sterilized de-ionized water) and incubate for 5-10 min in the dark.
18. Image the cells with an upright microscope with a 20x dip-in lens.
19. Take 50 images per device.
20. Process the images using an ImageJ plugin called Directionality.
    NOTE: Directionality options: This study used n = 45 bins, ranging from 0° to 176° to prevent a wrapping effect. The method employed was local gradient orientation, and the display table was selected. The direction output corresponds to the mean vector angle (indicating the angle of alignment), while the goodness output represents the mean vector length (indicating the degree of alignment).

2. Live cell imaging
   NOTE: Live cell imaging enables the tracking of dynamic cellular processes in real-time while keeping the cells in their natural, living state. This technique involves using a fluorescence microscope equipped with an incubation chamber to capture high-resolution images or videos of cells as they grow, divide, or respond to stimuli. Enabling the study of cellular behavior and interactions over time and providing valuable insights into cellular function and dynamics.
   1. Incubate the cells with SiR-actin 1:1000 ratio with culture media for 1 h at 37 °C.
   2. Aspirate the media and replace it with 1:2000 (SiR-actin: Media).
      NOTE: This dilution is to reduce cell toxicity for extended live imaging.
   3. Collect immunofluorescence images every 15 min for 5 h on an upright microscope with an incubation chamber, automated stage, and 20x dip-in lens.
      NOTE: For the live cell imaging experiment, the magnet was added as soon as the MRE was placed in the live imaging system.

Representative Results

Ultra-soft silicone-based magnetorheological elastomers (MREs) have elastic moduli that can be precisely tuned by applying a magnetic field. This allows for rapid, bi-directional adjustments within a physiological range, with precise control over both the rate and magnitude of changes (**Figure 1**). Gel mechanics were evaluated by measuring the elastic modulus as previously described, and the average elastic modulus was found to be 36.3 ± 5.2 kPa with magnet and 9.3 ± 1.2 kPa without magnet for the softer dynamic range MRE while the stiffer MRE ranges from 51.3 ± 7.0 kPa with magnet and 40.2 ± 3.7 kPa without magnet (**Figure 1**)[30,33,34]. MRE micro-patterns were created using a molding technique with a commercial diffraction grating, with features approximately 5.5 µm tall and 10 µm in pitch (distance between peaks). **Figure 2** shows plots comparing the normalized feature height of the master mold and MRE substrate, as well as the mean feature height and pitch. The average pitch was approximately 10 µm for the master mold and the final MRE culture substrate. The average feature size across the surface was 3.81 ± 0.59 µm for the final MRE and 5.49 ± 0.84 µm for the master mold.

The device fabrication technique presented here (**Supplementary Figure 1**) enables both the patterning of the culture substrate and dynamic modulation of stiffness, allowing for the investigation of the effects of ECM anisotropy and varying stiffness on cardiomyocyte alignment. For the cell

culture experiments, we conducted two primary experiments: matrix stiffening and softening. Stiffness was modulated by adding or removing a disc magnet (axially magnetized N45 neodymium rare earth magnet) 24 h post-seeding to induce stiffening or softening, respectively. Images were then captured at 3 h and 24 h after the stiffness change (stiffening or softening). At each time point, samples were stained to visualize and analyze morphological phenotypes (**Figure 3A**).

We then compared cardiomyocyte phenotypes seeded on patterned and flat substrates under matrix stiffening and softening conditions, as illustrated in the representative images in **Figure 3B**. Striking differences are evident across the groups, with cardiomyocytes appearing most aligned on the soft patterned substrate and most disorganized on the stiff unpatterned surface. Notably, cell alignment is influenced by both the substrate patterning and matrix stiffness, with the softer, patterned substrates promoting greater alignment of the cardiomyocytes. This underscores the critical roles of both mechanical and topographical cues in guiding the alignment of neonatal rat cardiomyocytes.

To further explore these differences, we quantified cell alignment during matrix stiffening and softening using two metrics: the alignment angle (mean vector angle, MVA) and the degree of alignment (mean vector length, MVL). The alignment angle ($-90° < \theta < 90°$) represents the orientation of cells relative to the horizontal axis. Visual inspection of the alignment angle on unpatterned surfaces for both stiffening and softening events reveals a broad distribution of angles between −90° and 90° and increased variability, which is expected as the cells are more disorganized. While the patterned surfaces show a clear bias toward an alignment angle of 0° (**Figure 3C**). Over time, there is increased variability post-stiffening or softening, likely indicating that the complete remodeling or organization process takes longer than the timeline of the experiment presented here. These observations were further validated through statistical comparisons (t-tests) between groups for both stiffening and softening conditions, as summarized in **Supplementary Table 1**.

As a complementary analysis, we examined the degree of alignment that quantifies how well features are aligned with each other. The degree of alignment ranges from 0 to 1, with a value of 1 indicating greater horizontal alignment. Cardiomyocytes on patterned substrates with matrix stiffening showed a decrease in alignment over time compared to the control. In contrast, the matrix softening condition led to an increase in alignment over time compared to the control (**Figure 3C**). These findings were confirmed by ANOVA followed by Tukey's post-hoc tests, which revealed significant differences between the temporal patterned substrates and the control, as detailed in **Supplementary Table 2**.

We extend temporal experimentation by optimizing the use of our materials to track individual cardiomyocytes over time using live-imaging probes. This method not only allows for the continuous monitoring of cellular behavior but also enables direct visualization of subcellular remodeling in response to changing environmental conditions. By capturing dynamic cellular processes in real-time, we can observe how cardiomyocytes adapt and reorganize at both the cellular and molecular levels. Using patterned MREs, we track the response of cardiomyocytes to stepwise changes in mechanical properties (**Supplementary Video 1**).

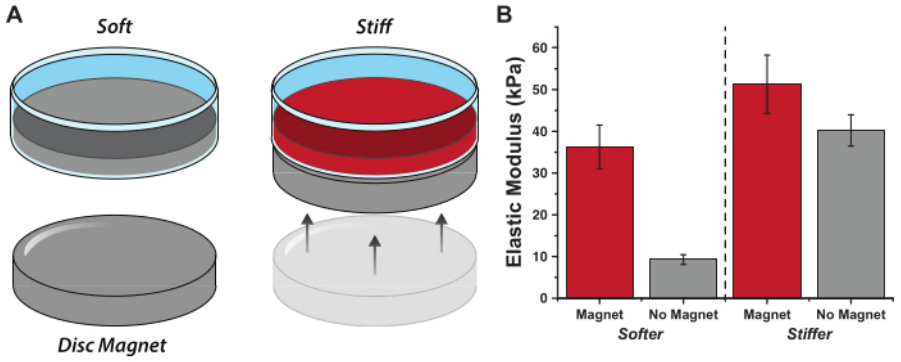

Figure 1: Overview of the magnetorheological elastomer. (**A**) Mechanism of stiffening - by applying an external magnetic field, the MRE will stiffen. (**B**) Microindentation results show the mechanical differences between the magnet and no magnet conditions for both softer and stiffer physiological ranges. Please click here to view a larger version of this figure.

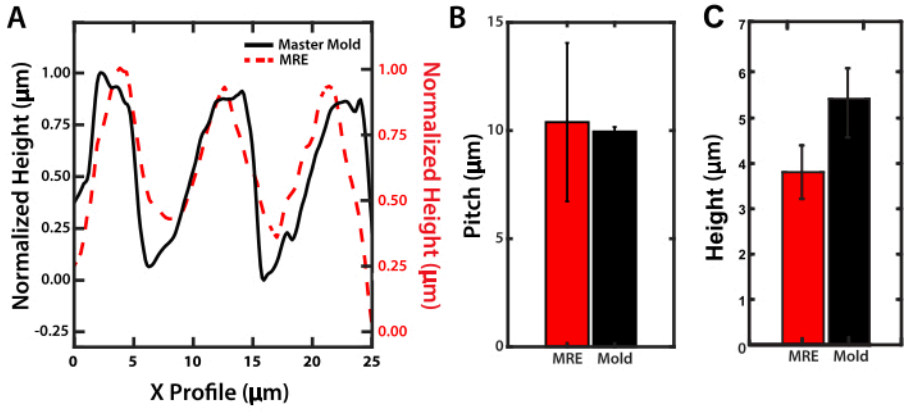

Figure 2: Overview of transferred topographic features onto MRE surfaces. Surface characterization was performed using laser confocal imaging (Keyence VK-X3000) and post-processing via open software Gwyddion. (**A**) The graph on the left shows the pitch values across the MRE (dashed red) and master mold (black) over the same length scale. (**B**) The average pitch for the MRE (red) and master mold (black). (**C**) The average feature height for the MRE (red) and master mold (black). Please click here to view a larger version of this figure.

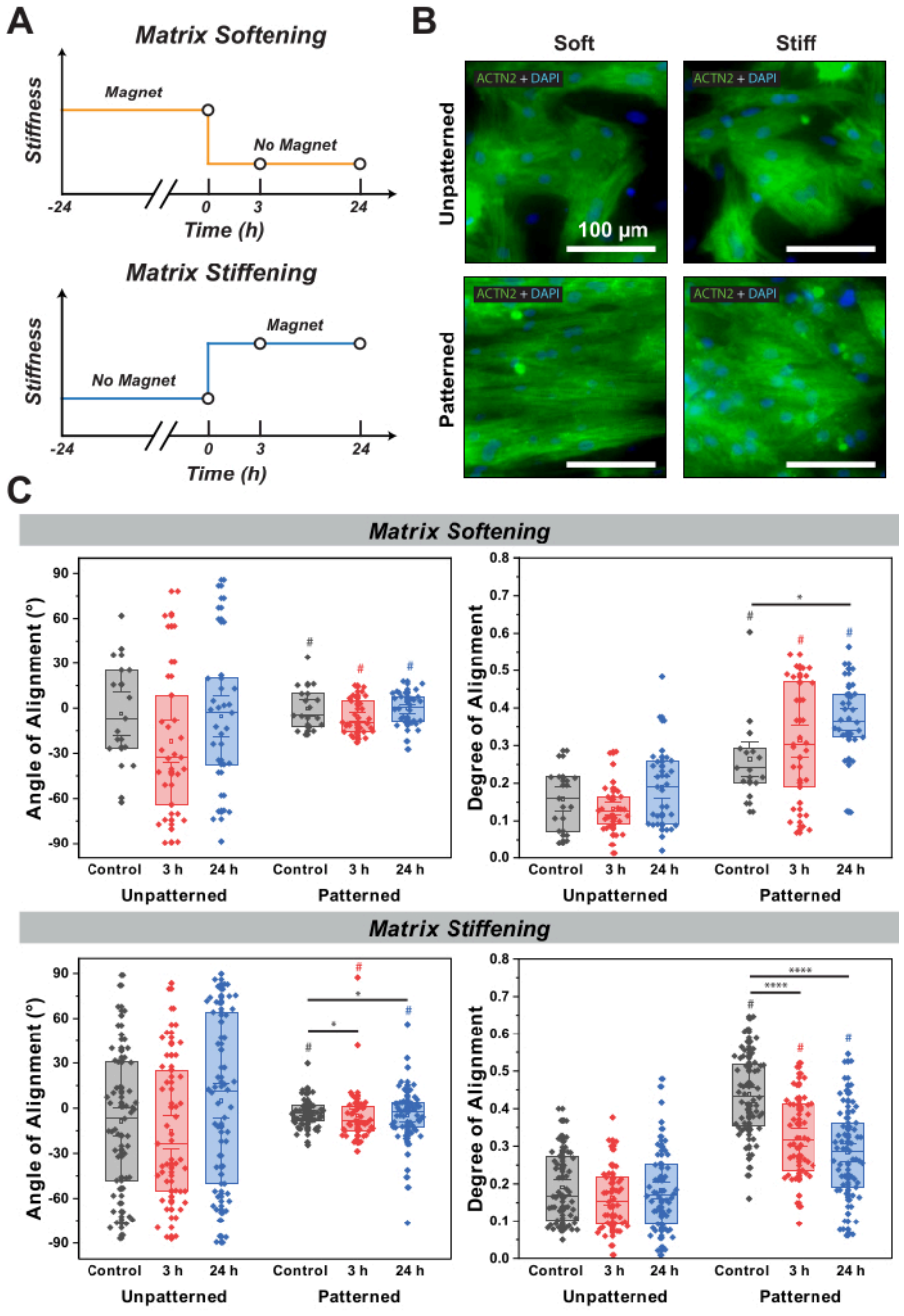

Figure 3: Cell alignment characterization under temporal changes in substrate stiffness. (**A**) Schematic illustration of temporal tests for matrix-stiffening and matrix-softening conditions. (**B**) Representative images of neonatal rat cardiomyocytes on unpatterned and patterned surfaces that were either stiff or soft. (**C**) Quantification of cell alignment and degree of alignment for a temporal stiffening or softening event. (# represents significance ($p < 0.05$) between unpatterned

and patterned. * represents significance ($p < 0.05$) over time. **** represents significance ($p < 0.005$) over time.) Please click here to view a larger version of this figure.

Supplementary Figure 1: Process for Creating Surface Features on MREs. A diffraction grating (master mold) is pressed into partially cured 184 PDMS and baked, then removed. The 184 PDMS surface is plasma-treated and silanized for easy MRE removal, and the stamp is cut to size. MRE material is poured onto the stamp, which is then flipped and applied to partially cured MRE in a dish. After baking, the stamp is removed, leaving behind the diffraction grating features on the surface of the MRE. Please click here to download this File.

Supplementary Video 1: Live imaging time-lapse video of neonatal rat cardiomyocytes on micro-patterned MRE responding to substrate stiffening. Neonatal rat cardiomyocytes seeded onto a stiffer MRE. After 24 h of culture with no magnet (soft condition), a magnet is applied at t = 0 h, the video starts at t = 2 h, and images are taken every 15 min. Please click here to download this File.

Supplementary Table 1: Statistical results of angle of alignment and degree of alignment between groups for both stiffening and softening conditions. Data displayed at mean ± SD. p-values are from Tukey's post-hoc analysis. Please click here to download this File.

Supplementary Table 2: Statistical results of angle of alignment and degree of alignment between patterned and unpatterned. Data displayed at mean ± SD. p-values are from Tukey's post-hoc analysis. Please click here to download this File.

Discussion

This technique has been rigorously tested, but careful attention to several steps is essential for a successful experiment.

In this protocol, we use a commercial diffraction grating as the master mold for patterning. However, alternative patterned molds-such as silicon or SU8 micro-manufactured molds-can also be employed to create a wide variety of patterns in different sizes[33,35]. Some commercially available PDMS materials come pre-patterned[36,37], which can also serve as an effective stamp for patterning the mechanoregulatory environments. While a speed mixer simplifies the process of mixing PDMS or silicone with carbonyl iron particles, the same result can be achieved by combining hand mixing with vortexing the solution for approximately twice the duration used with the speed mixer.

Many laboratories may not have access to a plasma O_2 cleaner, so we provide an alternative surface treatment for easier separation of the PDMS stamp. Instead of using a silane treatment, a mixture of isopropyl alcohol (IPA) and common dish soap can be used effectively. This modification involves preparing a solution of 2 parts IPA to 1 part dish soap, which we have found to be a reliable method. The soap solution is applied to the PDMS stamp and left to soak for 30 min. After soaking, the stamp should be dried with nitrogen gas before applying the MRE. This treatment facilitates easier release of the stamp from the sticky MRE. However, it is crucial to remove the stamp in the direction of the pattern to avoid disrupting the pattern's integrity.

The reagent ratios for fabricating the MREs can be adjusted based on the specific requirements of the device (**Table 1**). The ratio of carbonyl iron particles to elastomer, for example, influences the extent of stiffness change upon the application or removal of a magnetic field[34]. Varying this ratio allows for tuning the responsiveness of the MRE. In a study by Clark et al., it has been shown that increasing the volume fraction of iron particles from 9% to 23% led to an increase in the stiff (magnet) condition of the MREs from ~18 kPa to ~102 kPa[34]. Varying the distance between the magnetic field and MRE also adds another level of tunability, as shown by Corbin et al., the storage modulus (G') can be decreased from 20 kPa with no spacer (175.4 mT) to ~8 kPa with the addition of an 8mm spacer (91.2 mT)[30]. The stiffness ranges for the softer MRE were chosen to be both physiologically relevant, ~10 kPa without magnetic stimulation, and pathophysiologically relevant, ~35 kPa with magnetic stimulation, for native heart tissue. Additionally, alternative silicone-based elastomers, such as the Eco elastomer[33], can be used instead of traditional 527 PDMS[34]. The Eco elastomer-based MREs can be further tailored by adjusting the amount of silicone thinner, yielding softer or stiffer substrates depending on the application, with or without the influence of an external magnetic field. The success of the pattern transfer can be assessed using an upright microscope, as the material is opaque. Distinct differences between the peaks and valleys, along with the degree of parallelism, provide valuable indicators of the quality of the pattern transfer to the final MRE.

The application of magnetic fields to *in vitro* cultures often raises questions about potential changes in biological expression. However, we have previously established that, at the time scales used in our experiments and with the relatively low magnetic field strengths applied, there is no significant change in expression caused by the magnetic field[30].

While this technique was initially designed to study the effects of anisotropy and dynamic stiffness on cardiomyocyte organization and maturation, it is versatile and can be applied to various cell types and cellular processes. This platform is particularly useful for investigating processes like morphogenesis, angiogenesis, and fibrosis, which involve dynamic changes in cell structure and mechanical properties. Other groups have been utilizing MRE devices to investigate drug delivery for cancer therapy[38], tissue engineering in bone[39], and neuronal repair[40,41].

As mentioned, a limitation of this technique is the reliance on certain equipment, for example, a plasma O_2 cleaner to achieve high fidelity in transferred patterns. Although an alternative surface treatment can be used, this step is critical for achieving optimal results.

Patterned cell culture substrates have been in use for decades. However, the novelty of this platform lies in its ability to dynamically modulate substrate stiffness in addition to topographical patterning. This dual modulation of mechanical and topographical cues enables the study of dynamic cellular processes -- such as cell alignment, migration, and differentiation -- that were previously constrained to static stiffness environments with or without topographical guidance. This dynamic approach opens new avenues for investigating cellular behavior in a more physiologically relevant context.

Disclosures

The authors declare no conflicts of interest.

Acknowledgments

This research was partly supported by the Delaware Center for Musculoskeletal Research COBRE (P20 GM139760), with grants from the National Institute of General Medical Science from the National Institutes of Health and the State of Delaware. We would like to express our sincere gratitude to Sagar Doshi from the Center for Composite Materials (CCM) and Ashika Singh from the Dhong lab at the University of Delaware for their invaluable support in allowing us to use their laser confocal microscopes and for providing the expertise necessary for the surface characterization of our materials. Their contribution significantly enhanced the quality of our work.

References

1. Jacot, J. G., McCulloch, A. D., Omens, J. H. Substrate stiffness affects the functional maturation of neonatal rat ventricular myocytes. *Biophys J.* **95** (7), 3479-3487 (2008).
2. Körner, A., Mosqueira, M., Hecker, M., Ullrich, N. D. Substrate stiffness influences structural and functional remodeling in induced pluripotent stem cell-derived cardiomyocytes. *Front Physiol.* **12**, 710619 (2021).
3. Dou, W. et al. A microdevice platform for characterizing the effect of mechanical strain magnitudes on the maturation of iPSCcardiomyocytes. *Biosens Bioelectron.* **175**, 112875 (2021).
4. Abadi, P. P. S. S. et al. Engineering of mature human induced pluripotent stem cellderived cardiomyocytes using substrates with multiscale topography. *Adv Funct Mater.* **28** (19), 1707378 (2018).
5. Ahn, H. et al. Hierarchical topography with tunable micro and nanoarchitectonics for highly enhanced cardiomyocyte maturation via multiscale mechanotransduction. *Adv Healthc Mater.* **12** (12), 2202371 (2023).
6. Chan, Y.C. et al. Electrical stimulation promotes maturation of cardiomyocytes derived from human embryonic stem cells. *J Cardiovasc Transl Res.* **6** (6), 989-999 (2013).
7. Hirt, M. N. et al. Functional improvement and maturation of rat and human engineered heart tissue by chronic electrical stimulation. *J Mol Cell Cardiol.* **74**, 151-161 (2014).
8. Levental, I., Georges, P. C., Janmey, P. A. Soft biological materials and their impact on cell function. *Soft Matter.* **3** (3), 299-306 (2007).
9. Swift, J. et al. Nuclear laminA scales with tissue stiffness and enhances matrixdirected differentiation. *Science.* **341** (6149), 1240104 (2013).
10. Isermann, P., Lammerding, J. Nuclear mechanics and mechanotransduction in health and disease. *Curr Biol.* **23** (24), R1113-R1121 (2013).
11. Wozniak, M. A., Chen, C. S. Mechanotransduction in development: a growing role for contractility. *Nat Rev Mol Cell Biol.* **10** (1), 34-43 (2009).
12. Yang, X., Pabon, L., Murry, C. E. Engineering adolescence. *Circ Res.* **114** (3), 511-523 (2014).
13. Hazeltine, L. B. et al. Effects of substrate mechanics on contractility of cardiomyocytes generated from human pluripotent stem cells. *Int J Cell Biol.* **2012**, 508294 (2012).
14. Discher, D. E., Janmey, P., Wang, Y. Tissue cells feel and respond to the stiffness of their substrate. *Science.* **310** (5751), 1139-1143 (2005).

15. Deng, B., Zhao, Z., Kong, W., Han, C., Shen, X., Zhou, C. Biological role of matrix stiffness in tumor growth and treatment. *J Transl Med.* **20** (1), 540 (2022).

16. Jaalouk, D. E., Lammerding, J. Mechanotransduction gone awry. *Nat Rev Mol Cell Biol.* **10** (1), 63-73 (2009).

17. Vite, A. et al. Extracellular stiffness induces contractile dysfunction in adult cardiomyocytes via cellautonomous and microtubuledependent mechanisms. *Basic Res Cardiol.* **117** (1), 41 (2023).

18. Stowers, R. S. et al. Matrix stiffness induces a tumorigenic phenotype in mammary epithelium through changes in chromatin accessibility. *Nat Biomed Eng.* **3** (12), 1009-1019 (2019).

19. Engler, A. J. et al. Embryonic cardiomyocytes beat best on a matrix with heartlike elasticity: scarlike rigidity inhibits beating. *J Cell Sci.* **121** (22), 3794-3802 (2008).

20. Rodriguez, A. G., Han, S. J., Regnier, M., Sniadecki, N. J. Substrate stiffness increases twitch power of neonatal cardiomyocytes in correlation with changes in myofibril structure and intracellular calcium. *Biophys J.* 101 (10), 2455-2464 (2011).

21. Boothe, S. D. et al. The effect of substrate stiffness on cardiomyocyte action potentials. *Cell Biochem Biophys.* **74** (4), 527-535 (2016).

22. Curtis, A., Wilkinson, C. Topographical control of cells. *Biomaterials.* **18** (24), 1573-1583 (1997).

23. Martínez, E., Engel, E., Planell, J. A., Samitier, J. Effects of artificial micro and nanostructured surfaces on cell behaviour. *Ann Anat.* **191** (1), 126-135 (2009).

24. Ravichandran, R., Liao, S., Ng, C. C., Chan, C. K., Raghunath, M., Ramakrishna, S. Effects of nanotopography on stem cell phenotypes. *World J Stem Cells.* **1** (1), 55 (2009).

25. Brunetti, V. et al. Neurons sense nanoscale roughness with nanometer sensitivity. *Proc Natl Acad Sci U S A.* **107** (14), 6264-6269 (2010).

26. Clark, P., Connolly, P., Curtis, A. S. G., Dow, J. A., Wilkinson, C. D. Topographical control of cell behaviour: I. Simple step cues. *Development.* **99** (3), 439-448 (1987).

27. Nguyen, A. T., Sathe, S. R., Yim, E. K. F. From nano to micro: topographical scale and its impact on cell adhesion, morphology and contact guidance. *J Phys Condens Matter.* **28** (18), 183001 (2016).

28. DowellMesfin, N. M. et al. Topographically modified surfaces affect orientation and growth of hippocampal neurons. *J Neural Eng.* **1** (2), 78-90 (2004).

29. Loesberg, W. A. et al. The threshold at which substrate nanogroove dimensions may influence fibroblast alignment and adhesion. *Biomaterials.* **28** (27), 3944-3951 (2007).

30. Corbin, E. A. et al. Tunable and reversible substrate stiffness reveals a dynamic mechanosensitivity of cardiomyocytes. *ACS Appl Mater Interfaces.* **11** (23), 20603-20614 (2019).

31. Bouhrira, N., Vite, A., Margulies, K. B. Distinct cytoskeletal regulators of mechanical memory in cardiac fibroblasts and cardiomyocytes. *Basic Res Cardiol.* **119** (2), 277-289 (2024).

32. Lee, B. W. et al. Adult human cardiomyocyte mechanics in osteogenesis imperfecta. *Am J Physiol Heart Circ Physiol.* **325** (4), H814-H821 (2023).

33. Cao, Z., Ball, J. K., Lateef, A. H., Virgile, C. P., Corbin, E. A. Biomimetic substrate to probe dynamic interplay of topography and stiffness on cardiac fibroblast activation. *ACS Omega.* **8** (6), 5406-5414 (2023).

34. Clark, A. T. et al. Magnetic field tuning of mechanical properties of ultrasoft PDMSbased magnetorheological elastomers for biological applications. *Multifunct Mater.* **4** (3), 035001 (2021).

35. Kim, Y., Kwon, C., Jeon, H. Genetically engineered phage induced selective H9c2 cardiomyocytes patterning in PDMS microgrooves. *Materials.* **10** (8), 973 (2017).

36. Fujiwara, Y., Deguchi, K., Miki, K., Nishimoto, T., Yoshida, Y. A method for contraction force measurement of hiPSCderived engineered cardiac tissues. *Methods Mol Biol.* **2320**, 171-180 (2021).

37. Dirar, Q. et al. Activation and degranulation of CART cells using engineered antigenpresenting cell surfaces. *PLoS One.* **15** (9), e0238819 (2020).

38. Kim, C., Kim, H., Park, H., Lee, K. Y. Controlling the porous structure of alginate ferrogel for anticancer drug delivery under magnetic stimulation. *Carbohydr Polym.* **223**, 115045 (2019).

39. Fan, D. et al. Recent advances of magnetic nanomaterials in bone tissue repair. *Front Chem.* **8**, 745 (2020).

40. GonzalezRico, J. et al. Tuning the cell and biological tissue environment through magnetoactive materials. *Appl Sci.* **11** (18), 8746 (2021).

41. AntmanPassig, M., Shefi, O. Remote magnetic orientation of 3D collagen hydrogels for directed neuronal regeneration. *Nano Lett.* **16** (4), 2567-2573 (2016).